NMR Verification of Single Droplet Freezing Models

J. P. Hindmarsh, D. I. Wilson, and M. L. Johns
Dept. of Chemical Engineering, University of Cambridge, Cambridge, CB2 3RA, U.K.

A. B. Russell
Unilever Research, Colworth House, Sharnbrook, Bedford, MK44 1LQ, U.K.

X. D. Chen
Dept. of Chemical and Materials Engineering, University of Auckland, Auckland, New Zealand

DOI 10.1002/aic.10521
Published online July 7, 2005 in Wiley InterScience (www.interscience.wiley.com).

Acquiring temporal solid/liquid fraction data of a freezing system is advantageous for verifying theoretical solidification models. Nuclear magnetic resonance (NMR) spectrometry was used to obtain liquid fraction data of droplets of either water or sucrose solution undergoing freezing. The data obtained were used to verify numerical models of this solidification process. For water droplets, good agreement was observed between the experimental and model predictions of the temporal change in the water fraction over the range of air temperatures studied, whereas for the sucrose solution good agreement was observed only at the highest air temperature. At lower air temperatures, the discrepancies of the model were attributed to the possible crystallization of sucrose at temperatures above its reported glass-transition temperature. © 2005 American Institute of Chemical Engineers *AIChE J,* 51: 2640–2648, 2005
Keywords: NMR, freezing, droplets, modeling, solidification

Introduction

Analysis of the solidification of a droplet is of major importance in the study of spray-freezing processes. Spray freezing can be simply described as the solidification of a liquid by atomization into a relatively cold atmosphere.[1] It is a process developed for the production of powder from a range of materials such as foodstuffs,[1] metals,[2] the cryogenic preservation of cells,[3] pharmaceuticals,[4] the crystallization of ammonium nitrate,[5] and the artificial production of snow.[6] Being able to predict the freezing times and temperature transition of a single droplet is essential for optimization of spray-freezing processes.

Correspondence concerning this article should be addressed to M. L. Johns at mlj21@cheng.cam.ac.uk.

The literature contains many examples of the numerical modeling of the solidification of droplets. Previous studies have dealt with the freezing of water droplets[6-9] and foodstuffs[10] but the major body of work has focused on the solidification of metal droplets.[11-16] In all of these studies experimental data were not available to validate the performance of any model at predicting the temporal change in the solid/liquid fraction within the freezing/solidifying droplet.

In general, to measure the temporal change in the solid/liquid fraction during freezing, optical observation of freezing in thin plates,[17] thermograms,[18] and differential scanning calorimetry (DSC) can be used. These methods, however, are not amenable to studies of droplets, either free-falling or suspended, because they cannot readily accommodate such a geometry and they also generally require larger sample sizes. With nuclear magnetic resonance (NMR) spectrometry it is possible to calculate the liquid fraction from the magnetic

resonance ^{1}H signal intensity. This is related to the mass of liquid solution present in a sample volume because a frozen solution gives a negligibly small NMR signal. Previous NMR studies of freezing phenomena[19,20] used time-resolved NMR to monitor the freezing of apples and potatoes, using the data acquired to verify theoretical models.

In this work, the freezing of both water and sucrose solution droplets, suspended from a fine capillary, was investigated using time-resolved NMR. Sucrose solution was used as a model food because it has industrial application as a common sweetener in food products. It also has well-defined NMR properties, and its freezing characteristics in droplet form have been investigated previously.[21]

Background

Droplet freezing

Figure 1 shows the typical temperature transitions observed in a water (Figure 1a) and a 20 wt % sucrose solution (Figure 1b) droplet with diameters of 2 mm (suspended from a measuring thermocouple) as it freezes in a cooling air flow.[21] The droplet freezing process can be described by five distinct stages:

Stage (i): Liquid Cooling and Supercooling. The stage during which the liquid droplet is cooled from its initial state to a temperature below the equilibrium freezing point.

Stage (ii): Nucleation. Stage in which there is sufficient supercooling for spontaneous crystal nucleation to occur.

Stage (iii): Recalescence. Stage during which supercooling drives rapid kinetic crystal growth from the crystal nuclei. There is an abrupt temperature rise because this growth liberates latent heat of fusion. This stage is terminated when the supercooling is exhausted and the droplet has reached an equilibrium freezing temperature.

Stage (iv): Freezing. Stage in which further growth of the solid phase is governed by the rate of heat transfer to the environment from the droplet. This process continues until the droplet is "completely " frozen. During this stage, progressively greater freezing point depression can arise as the result of an increased concentration of solutes in the unfrozen liquid phase.

Stage (v): Solid Cooling or Tempering. Stage during which the temperature of the solidified droplet reduces to a steady-state value near that of the ambient air.

Models will be formulated to predict the liquid fraction changes during the recalescence (iii) and freezing (iv) stages for water and sucrose solution droplets. The model predictions for the temporal change in the liquid fraction will be compared directly against the values measured with NMR for a range of freezing conditions.

Experimental

Sucrose solution preparation

A 20% w/w sucrose solution was prepared with sucrose (99.5%) from Sigma Laboratory Supplies. This was dissolved in distilled water, shaken in a bottle, and left overnight before use.

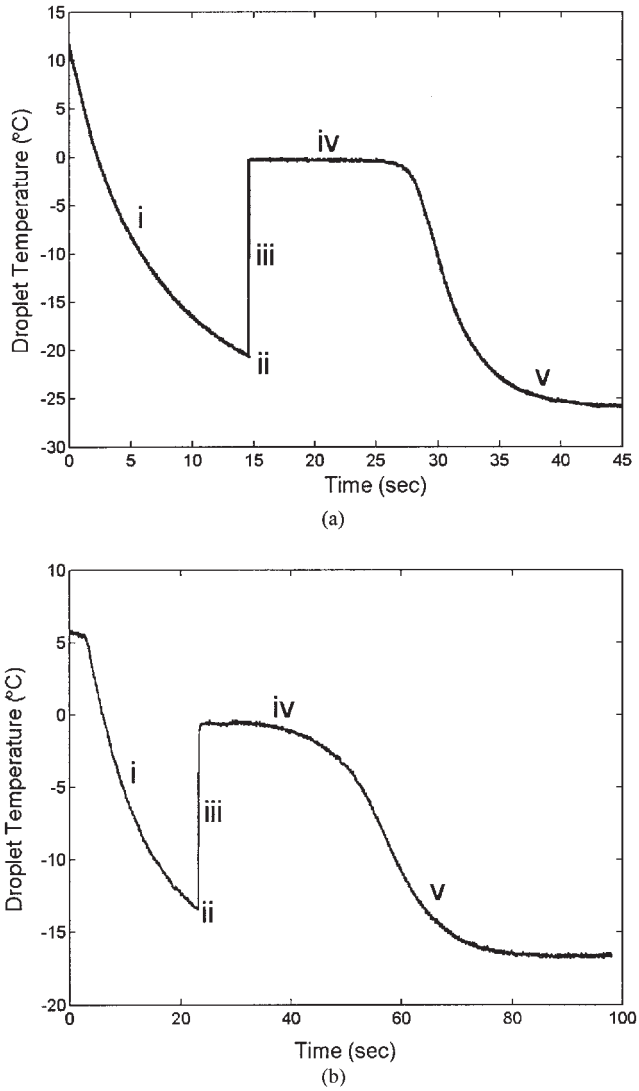

Figure 1. Temperature transitions of freezing droplets in airflow, illustrating: (i) supercooling, (ii) nucleation, (iii) recalescence, (iv) heat-transfer–governed freezing, and (v) tempering.

(a) Water; (b) sucrose solution.[21]

Differential scanning calorimetry

The thermal behavior of 20 wt % sucrose solution subjected to 5, 10, and 20°C/min cooling conditions was measured using a Perkin–Elmer power-compensated differential scanning calorimeter (DSC) equipped with nitrogen cooling. Samples of about 4 mg were hermetically sealed in standard aluminum DSC pans and scanned from 25 to −40°C.

Experimental apparatus

Magnetic resonance experiments were performed using a Bruker DMX 300 spectrometer featuring a 7.14-T vertical-bore magnet fitted with either a 5- or 10-mm-diameter ^{1}H birdcage radio frequency (RF) coil and a Bruker BVT 3000 temperature-control unit. The temperature of the air was

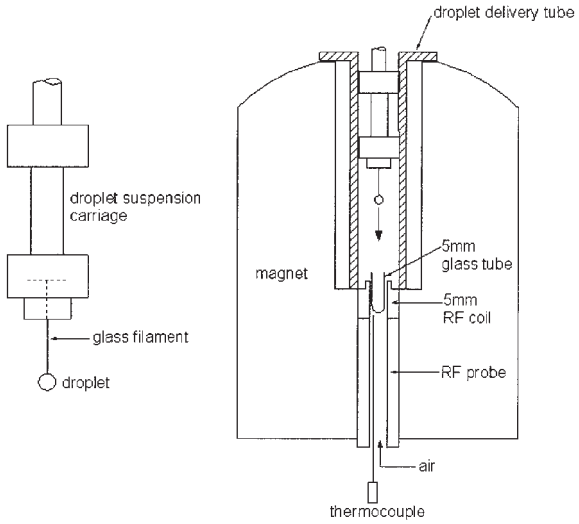

Figure 2. Experimental rig used for single-droplet suspension and delivery into a vertical bore magnetic resonance spectrometer.

controlled by a T-type thermocouple connected to the Bruker BVT 3000 and a cold airflow supplied from beneath the magnet.

A schematic of the experimental rig used to deliver and suspend a droplet inside the spectrometer magnet is shown in Figure 2. The principle is that a Perspex® tube is inserted into the top of the magnet bore, which acts as a guide to deliver the Perspex® drop suspension carriage to the top of the RF coil. The carriage has an approximately 2-mm-diameter droplet suspended from the tip of a fine glass filament (~50 μm diameter) and is prefitted to rest on top of the RF coil, with the drop located in the center of the RF coil.

Time-resolved NMR spectra

To monitor the droplet freezing, time-resolved ^{1}H spectra were acquired by exciting the ^{1}H spins in the sample with a 90° RF pulse and acquiring the signal at a time $t = 20$ μs after the 90° pulse. Because the spin–spin relaxation time (T_2) of the frozen components (water and sucrose) is about 5 μs, the magnetization of the frozen protons will have almost completely decayed after 20 μs, whereas the decay of the magnetization of the unfrozen components will be negligible, essentially representing only a sampled signal from the unfrozen material in the droplet. The resultant NMR spectra contain distinct water and sucrose peaks, the areas of which enable the relative amount of these unfrozen materials to be quantified; these are hereafter referred to as (normalized) peak areas for water and sucrose, respectively. Spectra were continuously sampled after inserting the droplet into a constant air temperature environment until freezing stopped, at a time resolution or repetition time (T_R) of 1.2 s.

For the repetition time (T_R), the magnitude of the ^{1}H signal (S) from the 90° pulse will be

$$S = k\varphi\left[1 - \exp\left(-\frac{T_R}{T_1}\right)\right] \tag{1}$$

where k is a proportionality constant, φ is the density of ^{1}H spins in the sample, and T_1 is the spin–lattice relaxation time of the ^{1}H. The spin–lattice relaxation time (T_1) of the liquid is dependent on the temperature (the dependency of T_1 on temperature in supercooled water droplets has been published[22]); there will consequently be a change in the ^{1}H signal during the recalescence and freezing stages as a result of the formation of a solid fraction and a change in the liquid region temperature. For recalescence, assuming the solid fraction formation and temperature rise occurs within the repetition time (T_R), the unfrozen water fraction (f_w) remaining after recalescence can be calculated with

$$f_w = \frac{S_1}{S_0}\left\{\frac{1 - \exp\left[\frac{T_R}{T_{1(s)}}\right]}{1 - \exp\left[\frac{T_R}{T_{1(f)}}\right]}\right\} \tag{2a}$$

$$f_w = 1 - \frac{c_l\rho_l}{\rho_s}\left(\frac{T_f - T_s}{L_f}\right) \tag{2b}$$

where S_0 is the ^{1}H signal from the water at the supercooling temperature T_s (before recalescence); S_1 is the ^{1}H signal from the water after recalescence (assumed to be at the equilibrium freezing temperature of the liquid region T_f); and $T_{1(s)}$ and $T_{1(f)}$ are the ^{1}H spin–lattice relaxation times at the supercooling temperature (T_s) and at the initial equilibrium freezing temperature of the water (T_f), respectively. The origin of Eq. 2b is a simple energy balance where the heat absorbed by the droplet suddenly increasing its temperature from T_s to T_f [$c_l(T_f - T_s)$] is related, by the latent heat of freezing (L_f), to the amount of ice formed; this will be considered further below in our description of our numerical models. Because the supercooling temperature T_s is not known during the experiments, there are three unknowns in Eqs. 2a and 2b: f_w, $T_{1(s)}$, and T_s. The third required equation is the known relationship between T_1 and T (as shown in Hindmarsh et al.[22]). This enables an estimate of both f_w and $T_{1(s)}$, which is used in the model. For the freezing stage, the progressive change in the water fraction f_w is assumed to be directly proportional to the relative change in the ^{1}H signal; this assumes that the relative change in the freezing temperature between each acquisition is minimal.

Numerical Models

These experiments were performed under conditions described by small Biot numbers (<0.1), so that a simple lumped model for the droplet temperature can be used that does not account for heat conduction in the interior of the droplet and assumes that there is a uniform temperature distribution within the droplet during cooling and freezing. It has been postulated that with the occurrence of nonequilibrium solidification in rapidly freezing droplets the uniform temperature assumption was not valid,[23] even when the Biot number was <0.1. In previous work[8] it was found that the assumption of a uniform temperature profile in the droplet was justified and accurate for

the droplet sizes and freezing conditions used in this study. As a consequence, all models formulated to predict the freezing of water and sucrose solution droplets have used the uniform temperature assumption. This assumption means that temperature transition and freezing of the droplet can be solved by simply balancing the internal energy with the energy removed by convective heat transfer q_h, mass transfer q_m, and thermal radiation q_r from the surface of the droplet.

For the freezing process, the governing equations describing the internal heat balance of the droplet and the physical properties are discontinuous for recalescence (iii) and freezing (iv). It is therefore convenient to formulate a separate model for the internal energy balance of each stage.

Droplet surface heat fluxes

The convective heat flux q_h, from the droplet surface, is described by

$$q_h = h(T_{d,s} - T_a) \tag{3}$$

where h is the convective heat transfer coefficient; and $T_{d,s}$ and T_a are the droplet surface and the ambient air temperatures, respectively. The heat flux q_m, arising from convective mass transfer, is

$$q_m = Lh_m(a_w\rho_{d,vs} - \rho_{va}) \tag{4}$$

where L is the latent heat of phase change; h_m is the mass-transfer coefficient; and $\rho_{d,vs}$ and ρ_{va} are the droplet surface and air vapor densities, respectively. The addition of solutes typically decreases the rate of mass transfer from aqueous liquid or solid phases by decreasing the equilibrium vapor pressure at the surface. Water and ice can have associations with solutes. The term "water activity " (a_w) was developed to account for the intensity with which water associates with various solutes. At ambient pressures the water activity is defined as

$$a_w = \left(\frac{p}{p_0}\right) \tag{5}$$

where p is the partial vapor pressure of the solute containing solvent and p_0 is the partial vapor pressure of the pure solvent.[24] In the case of food solutions, the water activity is the partial vapor pressure at the surface of the food compared to that of pure water. The water activity a_w is used to adjust the saturated vapor pressure or vapor density at the droplet surface $\rho_{d,vs}$, in the convective mass transfer.[25]

For coupled heat and mass transfer from a sphere, the following correlations for the Nusselt number (Nu) and Sherwood number (Sh)[26,27] were used to estimate the heat- and mass-transfer coefficients h and h_m

$$\mathrm{Nu} \equiv \frac{2hR}{k_a} = 2 + 0.6\,\mathrm{Pr}^{1/3}\mathrm{Re}^{1/2} \tag{6}$$

$$\mathrm{Sh} \equiv \frac{2h_mR}{D_{ab}} = 2 + 0.6\,\mathrm{Sc}^{1/3}\mathrm{Re}^{1/2} \tag{7}$$

where R is the droplet radius, D_{ab} is the vapor–air diffusivity, k_a is the air thermal conductivity, and Re is the droplet Reynolds number. For flow past a sphere, the latter is given by

$$\mathrm{Re} = \frac{2R\rho_a\nu}{\mu_a} \tag{8}$$

where v, ρ_a, and μ_a are the air velocity, density, and viscosity, respectively. The Schmidt number (Sc) is

$$\mathrm{Sc} = \frac{\mu_a}{\rho_a D_{ab}} \tag{9}$$

and the Prandtl number (Pr) is given by

$$\mathrm{Pr} = \frac{\mu_a}{\rho_a\alpha_a} \tag{10}$$

where α_a is the thermal diffusivity of the air. For air below 0°C, Pr is approximately constant, at 0.7.[28]

The heat flux q_r arising from thermal radiation is

$$q_r = \varepsilon\sigma(T_{d,s}^4 - T_a^4) \tag{11}$$

where ε is the surface emissivity for thermal radiation and σ is the Stefan–Boltzmann constant for thermal radiation.

Recalescence stage

The small bodies of liquid contained in droplets means that large undercoolings, at the time of nucleation, can occur and a significant liquid fraction is consequently frozen during recalescence. To accurately predict the freezing time of a droplet, the solid fraction formed by recalescence needs to be incorporated into the numerical model. The temperature transition occurs extremely rapidly until the droplet reaches the equilibrium freezing temperature. A global heat balance can be used to estimate the liquid fraction remaining after recalescence. The mass of liquid frozen is such that the latent heat released raises the droplet temperature to the equilibrium freezing temperature T_f.[9,28] Therefore, the remaining liquid fraction f_l, after recalescence, is estimated by

$$f_l = 1 - \frac{c_l\rho_l}{\rho_s}\left(\frac{T_f - T_s}{L_f}\right) \tag{12}$$

where T_s is the nucleation temperature. On reaching T_s the droplet was assumed to instantly change to the equilibrium freezing temperature T_f with a fraction of the liquid frozen. For sucrose solutions, the solution heat capacity c_l and density ρ_l properties were those of the initial sucrose concentration. Also for sucrose solutions, the solid density ρ_s used was that of pure ice. This is because on a microscale, ice has approximately zero sucrose solubility.[29] Therefore, it is assumed that only pure ice is formed during recalescence. The sucrose concentration of the unfrozen liquid after recalescence is adjusted to account for the sucrose rejected during ice formation.

Freezing stage

During the freezing stage, assuming a uniform droplet temperature, the solid (frozen) volume V_f can be calculated from a simple heat balance

$$\frac{L_f \rho_s}{A}\frac{dV_f}{dt} = q_h + q_m + q_r \tag{13}$$

where A is the external surface area. For water, Eq. 13 was solved with a forward-difference time step. For each time step, the droplet size was updated to compensate for the loss of liquid resulting from mass transfer.

In the case of the sucrose droplets, the redistribution of the sucrose is described by the Scheil equation[30]:

$$\frac{C_l}{C_0} = \frac{1}{f_l^{(1-k_e)}} = \frac{1}{1 - f_s^{(1-k_e)}} \tag{14}$$

where C_0 is the initial solute concentration; C_l is the liquid region solute concentration; f_s and f_l are the solid and liquid volume fractions, respectively; and k_e is the equilibrium partition coefficient ($k_e = C_s/C_l$), where C_s is the solid region sucrose concentration. Because sucrose is almost insoluble in ice, in our simulations the equilibrium partition coefficient is assumed to be: k_e (and thus C_s) = 0.

The Scheil equation is incorporated into Eq. 13 to predict the solid/liquid segregation of the sucrose during freezing. This requires the following assumptions:

(1) The spacing between ice crystals is small enough so that there is no concentration gradient in the liquid.

(2) The freezing is ideal and at the equilibrium freezing temperature.

(3) Sucrose does not undergo crystallization.

The Scheil equation predicts the freeze concentration of the sucrose in the liquid region, which in turn was used to calculate the progressive freezing point depression (FDP) as the droplet freezes.

The heat-balance and Scheil equations (Eqs. 13 and 14) are solved with a forward-difference time step and the droplet size is again updated to compensate for the loss of liquid by mass transfer. For the time period $t + dt$, the change in the solid fraction $df_s^{(t+dt)}$ is calculated from the total heat flux from the droplet for the time step dt. The Scheil equation updates the change in the sucrose concentration in the liquid region $dC_l^{(t+dt)}$ for the change in solid fraction $f_s^{(t+dt)} + df_s^{(t+dt)}$. The new equilibrium freezing temperature is calculated as $T_{\mathrm{FPD}}[C_l^{(t-dt)} + dC_l^{(t+dt)}]$, where $T_{\mathrm{FPD}}(C_l)$ is a function predicting the freezing point depression for the sucrose concentration in the liquid region. The enthalpy required to cool the droplet from the old equilibrium freezing temperature [related to the liquid sucrose concentration in the preceding time step $C_l^{(t-dt)}$] to the new predicted equilibrium freezing temperature [related to the increased liquid sucrose concentration $C_l^{(t+dt)}$] is subtracted from the total heat flux used to calculate the new ice formed in the next time step $t + 2dt$. Once the droplet water is fully frozen ($f_l = 0$), the phase change stops and the model then operates as a solid droplet undergoing cooling.

For sucrose solution droplets, the mass transfer heat flux (q_m) is adjusted with values of the water activities (a_w) calculated from mass-transfer measurements.[21] It is assumed that the outer surface of the droplet remains liquid while freezing, so that mass transfer from the surface occurs by evaporation.

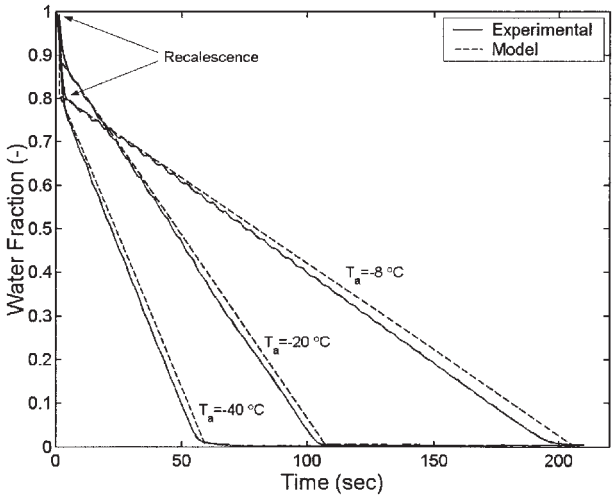

Figure 3. Comparison of model predictions for the time-resolved water fraction f_w to the NMR experimental data for 5-μL water droplets freezing in a range of air temperatures T_a.

All models were programmed in Matlab version 6.0 (The MathWorks, Natick, MA). To ensure that the numerical results were time-step independent, the time step was decreased until the solutions were stable, with <0.01% variation from the previous larger setting. A time step of 0.02 s was found to be optimal and was used for all models. The physical properties used for the simulations were taken from the appropriate literature.[28,31,32]

Results and Discussion

Water droplets

Figure 3 shows the comparison of the NMR experimental and predicted time-resolved data for the unfrozen water fraction f_w of 5-μL (2-mm-diameter) water droplets frozen over a range of cold air temperatures. The experimental and model results show good agreement. In validating the numerical model, this work demonstrates the potential of NMR for obtaining solid/liquid fraction data for verifying such theoretical solidification models.

Sucrose solution droplets

Figures 4a and 4b show the normalized peak area signal (each peak area divided by the maximum peak area) for the water and sucrose components in 20 wt % sucrose solution droplet as a function of time for a range of freezing temperatures. The freezing rate of the water component in Figure 4a is noticeably slower than the corresponding cases in Figure 3, which arises from the depression of the water freezing point because of the sucrose in solution. As freezing proceeds, the unfrozen water becomes more concentrated in sucrose, resulting in a further reduction in freezing rate. The signal from the water levels out at higher proportions as the air temperature

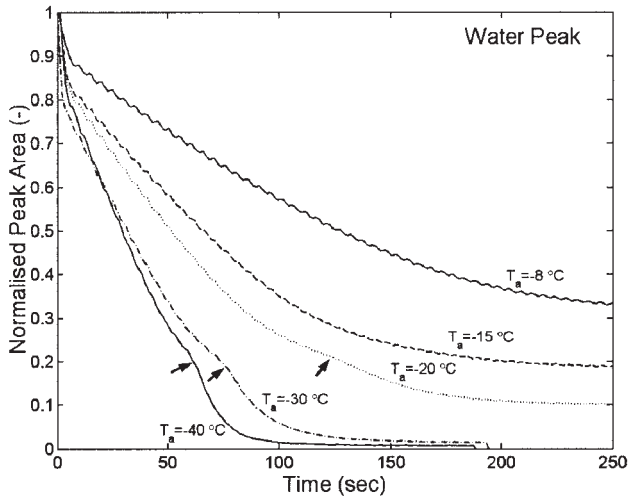

(a)

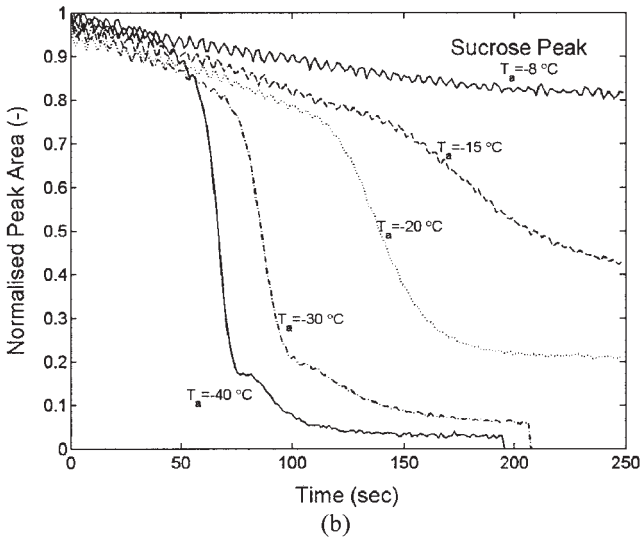

(b)

Figure 4. Time evolution of the normalized NMR peak area during freezing of 5-μL droplets of 20 wt % sucrose solution in a range of air temperatures T_a.

(a) Water peak; (b) sucrose peak.

increases, indicating that the sucrose solution is less maximally frozen.

In Figure 4b, for the sucrose signal, there are sudden rapid decreases for air temperatures ranging from −15 to −40°C and only a gradual decrease for the −8°C air temperature. The sharp decrease in the signal from the sucrose indicates that the sucrose has undergone a change in molecular mobility, which is possibly associated with the transformation to a glassy state. We speculate that this is potentially an intermediate stage before crystallization of the sucrose. The temporal freezing profiles for water and sucrose, presented in Figure 4, are combined for a freezing air temperature of −40°C in Figure 5. The phase change of the sucrose is accompanied with a reduction in the freezing rate of the water at a time of about 70 s (in Figure 5 an arrow indicates a discontinuity in the freezing rate of the water, which corresponds to the sudden loss of signal from the sucrose). It is thought that the latent heat liberated upon the phase change in the sucrose results in a reduction in freezing rate of the water.

This localized retardation of the water freezing rate was also observed for the droplets freezing in air at −20 and −30°C, as indicated by arrows in Figure 4a. At the same time, the evident decline in signal from the sucrose suggests that the sucrose is undergoing a phase change to a less mobile conformation. Both of the above air temperatures are higher than the reported mean glass-transition temperature of −32°C for sucrose solutions, which is reported to be independent of the initial sucrose concentration.[33] If the sucrose solution is not undergoing a glass transition, it suggests that the steep decrease in the signal could be a result of sucrose crystallization. This was not expected, given that the prevailing theory for sucrose solutions suggests that, as the temperature is lowered and the sucrose concentration increases, it is highly unlikely that sucrose will crystallize. The inhibition of crystallization is attributed to the solution viscosity increasing to the point where the mobility of sucrose is too low for nucleation of sucrose crystals to occur, so that there is no eutectic temperature and the sucrose remains in a nonequilibrium state as an amorphous liquid.[17,29,33-35]

DSC thermograms were taken of 20 wt % sucrose solution at the cooling rates of 5, 10, and 20°C/min. From the temperature-transition curves for sucrose solution droplets freezing in air temperatures ranging from −8 to −40°C the cooling rate during the freezing stage [see Figure 1b, stage (iv)] ranges from about 0 to 60°C/min. It is not possible for DSC to reproduce the maximum cooling rate but the cooling rates of 5, 10, and 20°C/min represent the range over which a majority of sucrose solution is frozen for air temperatures of −8 to −40°C.

The cooling thermograms for 20% sucrose solution for 5, 10, and 20°C/min are shown in Figure 6. The baselines of the scans have been offset for better comparison. It can be seen that high depths of undercooling occurred before the onset of freezing at all cooling rates, which is comparable to the behavior observed in sucrose solution droplets. The first peak for each thermogram (A) is likely to be the heat flow from the freezing of the

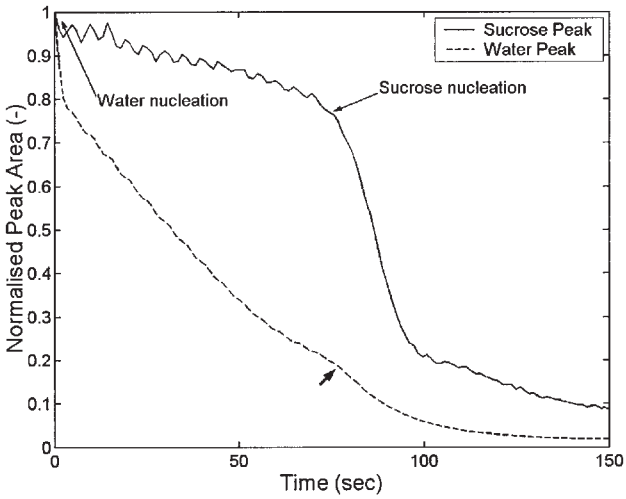

Figure 5. Time evolution of the normalized NMR peak area of the water and sucrose peaks during the freezing of a 5-μL 20 wt % sucrose solution droplet in air at −40°C.

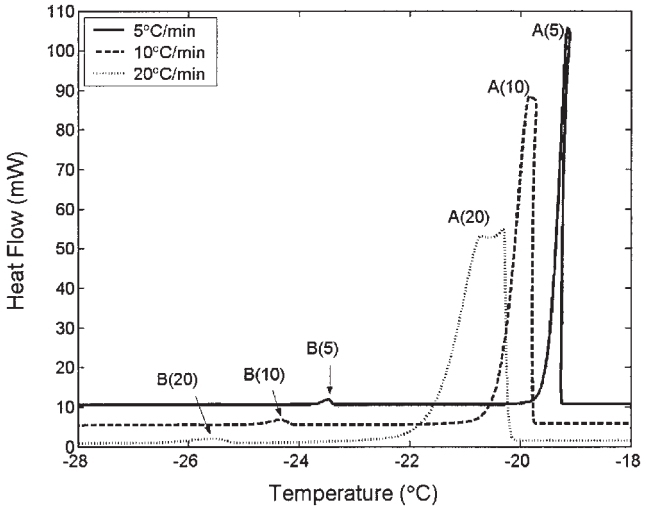

Figure 6. Cooling thermograms of the heat flow as a function of temperature for 20 wt % sucrose solution cooling from 25 to −40°C at 5, 10, and 20°C/min.

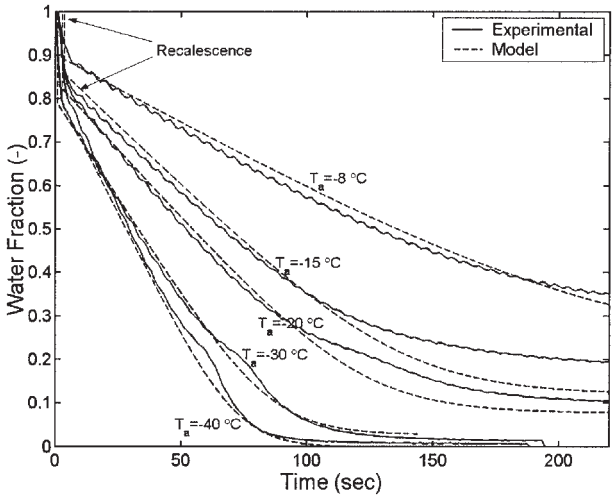

Figure 7. Comparison of model predictions to the NMR experimental data for the time resolved water fraction f_w of 5-μL 20 wt % sucrose solution droplets freezing in a range of air temperatures T_a.

water in the sucrose solution, although a second smaller peak (B) is evident at lower temperatures for each cooling rate. From the observations of phase change in the NMR results in Figure 4, it is possible that these second smaller peaks are the sucrose undergoing some phase change at temperatures higher than the expected glass-transition temperature of sucrose solutions.

The glass transitions of frozen sucrose solutions have been determined by use of differential scanning calorimetry (DSC) and scanning electron microscopy (SEM).[36] Investigators were particularly interested in what appeared to be double glass-transition temperatures in freezing sucrose solutions. They concluded that the apparent double glass-transition temperatures were caused by solute inclusions within the ice crystals that were formed from the rapid crystallization of water after deep undercooling of the sucrose solutions. The sucrose inclusions resulted in a system that showed complex relaxation in which both the bulk phase and the plasticized sucrose inclusions underwent a glass transition at different temperatures. It is possible that the concentrated sucrose inclusions do not undergo a glass transition but crystallize because it is possible that the sucrose inclusions reach concentration levels at temperatures where the sucrose is still sufficiently mobile to undergo nucleation and subsequent crystallization. This could explain the possible observation of sucrose crystallization in the freezing of the sucrose solution droplets, where deep undercoolings occur.

Figure 7 shows the comparison of the experimentally observed and the predicted water fraction content f_w during freezing of 20 wt % sucrose solution droplets over a range of air temperatures. For air temperatures ranging from −15 to −40°C, there are evident discrepancies between the experimental data and the model when the water fraction drops below 0.3. The model can be seen to overpredict the freezing rate of the water at lower air temperatures. This discrepancy in the frozen water fraction prediction manifests as an increasing underprediction in the temperature transition for the freezing sucrose solution droplet, as seen in Figure 8. This systematic difference was not evident at an air temperature of −8°C where there was good agreement for the water fraction and the temperature transition (compare Figures 7 and 8). It can also be seen in Figure 4b that for the −8°C air temperature there is no rapid drop in the signal from the sucrose, where this is evident for the air temperatures −15 to −40°C. The model assumes that only water freezes; it is thus likely that the systematic discrepancy in the model is explained by a level of crystallization of the sucrose.

Conclusions

Time-resolved NMR was used to gather experimental data of the temporal change in the water fraction of droplets undergo-

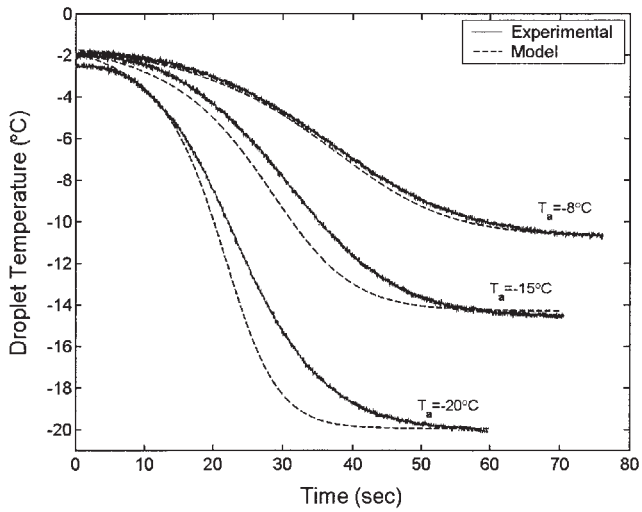

Figure 8. Comparison of the predicted and experimental temperature transitions of the freezing/solid cooling stages (iv and v) of 4-μL 20 wt % sucrose droplets freezing in a range of air temperatures T_a.

ing freezing for two model systems (water and sucrose solutions). The NMR results, which were supported by DSC analysis, suggested that some of the sucrose was undergoing a phase transition at a higher temperature than the glass-transition temperature of sucrose solutions. This unexpected phenomenon may be the product of deep undercooling of the sucrose solution. The rapid crystallization of ice crystals forms regions of concentrated sucrose inclusions within the matrix of the ice; in these regions the concentration reaches levels at temperatures where the sucrose is mobile enough to undergo nucleation and subsequent crystallization.

Simple numerical approaches were used to predict the temporal change of the water fraction in freezing water and sucrose droplets. It was assumed that there was no internal temperature gradient within the droplet and solidification was ideal. The results were compared against the NMR data. Good agreement was observed with the water droplets for all air temperatures but good agreement was observed with the sucrose solution droplets only at an air temperature of -8°C and for $f_w > 0.3$ for lower air temperatures. It was apparent that the discrepancy at lower air temperatures was the anomalous phase transition in sucrose. Some means of predicting the onset and quantity of crystallization of the sucrose must be incorporated into the model to improve the accuracy of predicting the freezing behavior of sucrose solution droplets.

To conclude, the results have demonstrated that NMR is a suitable method of gathering experimental data of the temporal change of the liquid fraction in a freezing system, which can be used to validate theoretical solidification models.

Acknowledgments

This work was supported by the Engineering and Physical Sciences Research Council (EPSRC) project GR/94800/01. The authors also acknowledge funding for J.P.H. from the APV Seligman Trust and the University of Auckland.

Notation

a_w = water activity
A = external surface area, m^2
c = specific heat capacity, J kg^{-1} K^{-1}
C = solute concentration, wt %
C_o = initial solute concentration, wt %
D_{ab} = air/water vapor diffusivity, m^2/s
f = fraction
h = heat-transfer coefficient, J sm^{-2} K^{-1}
h_m = mass-transfer coefficient, m/s
k = signal proportionality constant, kg
k_a = thermal conductivity, J sm^{-1} k^{-1}
k_e = equilibrium partition coefficient
L = latent heat of phase change, J kg^{-1}
Nu = Nusselt number
p = partial vapor pressure of solute containing solvent
p_0 = partial vapor pressure of pure solvent
Pr = Prandtl number
q = heat flux, J/m^2
r = radial coordinate, m
R = droplet radius, m
Re = Reynolds number
Sc = Schmidt number
S = proton signal
S_0 = proton signal at supercooling temperature
S_1 = proton signal after recalescence
Sh = Sherwood number
T_1 = spin–lattice relaxation time, s
t = time, s
T_2 = spin–spin relaxation time, s
$T_{1(f)}$ = spin–lattice relaxation time at freezing temperature, s
$T_{1(s)}$ = spin–lattice relaxation time at supercooling temperature, s
T_R = repetition time, s
T = temperature, K
T_s = supercooling temperature, °C
v = ambient air velocity, m/s
V_d = volume of droplet, m^3
V_f = volume of droplet frozen, m^3

Greek letters

α = thermal diffusivity, m^2/s
ε = emissivity
φ = density proton spins, kg^{-1}
μ = viscosity, Pa·s
ρ = density, kg/m
σ = Stefan–Boltzmann constant

Subscripts

a = ambient air
e = evaporation
d, s = droplet surface
FPD = freezing point depression function, K/wt %
f = fusion
h = heat transfer
l = liquid phase
m = mass transfer
n = nucleation
r = thermal radiation
s = solid phase
sb = sublimation
v = vapor phase
w = water

Literature Cited

1. Windhab EJ. New developments in crystallization processing. *J Therm Anal Calorim.* 1999;57:171-180.
2. Flemings MC. *Solidification Processing*. New York, NY: McGraw-Hill; 1974.
3. Fields SD, Strout GW, Russell SD. Spray-freezing apparatus for cryofixation of unicellular algae. *Proceedings of the 51st Annual Meeting of the Microscopy Society of America*. San Francisco, CA: San Francisco Press; 1993:134-135.
4. Leuenberger H. *New Technologies for the Manufacture of Nanostructured Drug Carriers*. London: World Markets Research Centre; 2001.
5. Filipescu L, Becherescu C, Radovici C, Doca I, Vasilescu G, Mocioaca G, Florea S. Nucleative prilling of ammonium-nitrate. *Rev Roum Chim.* 1992;37:777-784.
6. Liao JC, Ng KC. Effect of ice nucleators on snow making and spray freezing. *Ind Eng Chem Res.* 1990;29:361-366.
7. Gao W, Smith DW, Sego DC. Freezing behavior of freely suspended industrial waste droplets. *Cold Reg Sci Technol.* 2000;31:13-26.
8. Hindmarsh JP, Russell AB, Chen XD. Experimental and numerical analysis of the temperature transition of a suspended freezing water droplet. *Int J Heat Mass Transfer.* 2003;46:1199-1213.
9. Feuillebois F, Lasek A, Creismeas P, Pigeonneau F, Szaniawski A. Freezing of a subcooled liquid droplet. *J. Colloid Interface Sci.* 1995; 169:90-102.
10. Wilson HA, Singh RP. Numerical simulation of individual quick freezing of spherical foods. *Rev Int Froid.* 1987;10:149-155.
11. Epstein M, Fauske HS. Kinetic and heat transfer-controlled solidification of highly supercooled droplets. *Int J Heat Mass Transfer.* 1993;36:2987-2995.
12. Grant PS, Cantor B, Katgerman I. Modelling of droplet dynamic and thermal histories during spray forming: I. Individual droplet behaviour. *Acta Metall Mater.* 1993;41:3097-3108.
13. Lee E, Ahn S. Solidification progress and heat transfer analysis of gas-atomized alloy droplets during spray forming. *Acta Metall Mater.* 1994;44:3231-3243.
14. McCoy JK, Markworth AJ, Collings RS, Brodkey RS. Cooling and

solidification of liquid-metal drops in a gaseous atmosphere. *J Mater Sci.* 1992;27:761-766.
15. Su YH, Tsao CA. Modeling of solidification of molten metal droplet during atomization. *Metall Mater Trans B.* 1997;28B:1249-1255.
16. Wang GX, Matthys EF. Numerical modeling of phase change and heat transfer rapid solidification processes: Use of control volume integrals with element subdivision. *Int J Heat Mass Transfer.* 1992;35:141-153.
17. Muhr AH, Blanshard JMV. Effect of polysaccharide stabilizers on the rate of growth of ice. *J Food Technol.* 1986;21:683-710.
18. Faydi E, Andrieu J, Laurent P, Peczalski R. Experimental study and modelling of the ice crystal morphology of model standard ice cream. Part I: Direct characterization method and experimental data. *J Food Eng.* 2001;48:293-300.
19. Hills BP, Gincalves O, Harrison M, Godward J. Real time investigation of the freezing of raw potato by NMR microimaging. *Magn Reson Chem.* 1997;35:29-36.
20. Hills BP, Remigereau B. NMR studies of changes in subcellular water compartmentation in parenchyma tissue during drying and freezing. *Int J Food Sci Technol.* 1997;32:51-61.
21. Hindmarsh JP, Russell AB, Chen XD. Experimental and numerical analysis of the temperature transition of a freezing food solution droplet. *Chem Eng Sci.* 2004;59:2503-2515.
22. Hindmarsh JP, Wilson DI, Johns ML. Using MRI to predict the solid fraction formed during recalescence of freezing droplets. *Int J Heat Mass Transfer.* 2005;48:1017-1021.
23. Chang K, Chen C. Revisiting heat transfer analysis for rapid solidification of metal droplets. *Int J Heat Mass Transfer.* 2001;44:1573-1583.
24. Fennema OR. *Food Chemistry*. New York, NY: Marcel Dekker; 1996.
25. Delgado AE, Sun D-W. Heat and mass transfer models for predicting freezing processes—A review. *J Food Eng.* 2001;47:157-174.
26. Ranz WE, Marshall JWR. Evaporation from drops, Part II. *Chem Eng Prog.* 1952;48:173-180.
27. Incropera FP, DeWitt DP. *Fundamentals of Heat and Mass Transfer*. 4th Edition. New York, NY: Wiley; 1996.
28. Hobbs PV. *Ice Physics*. Oxford, UK: Clarendon Press; 1974.
29. Kantor Z, Jan Thoen GP. A model for freeze concentration and glass transition of carbohydrate solutions as determined by differential scanning calorimetry. *High Temp-High Press*. 2001;33:103-110.
30. Kurz W, Fisher DJ. *Fundamentals of Solidification*. Aedermannsdorf, Switzerland: Trans Tech Publications; 1992.
31. Bubnik Z, Kadlek P, Urban D, Bruhns M. *Sugar Technologists Manual: Chemical and Physical Data for Sugar Manufactures and Users*. Berlin: Bartens; 1995.
32. Perry RH, Green DW. *Perry's Chemical Engineer's Handbook*. New York, NY: McGraw-Hill; 1997.
33. Sahagian M, Goff HD. Effect of freezing rate on the thermal, mechanical and physical aging properties of the glassy state in frozen sucrose solutions. *Thermochim Acta.* 1994;246:271-283.
34. Hartley RH, Mant A. Determination of the unfrozen water content of maximally freeze concentrated carbohydrate solutions. *Int J Biol Macromol.* 1993;15:227-232.
35. Jeremiah LE. *Freezing Effects on Food Quality*. New York, NY: Marcel Dekker; 1995.
36. Goff HD, Versespej E, Jermann D. Glass transitions in frozen sucroses are influenced by solute inclusions within ice crystals. *Thermochim Acta.* 2003;399:43-55.

Manuscript received Feb. 17, 2004, and revision received Feb. 1, 2005.